1994PASP..106..642H

Publications of the Astronomical Society of the Pacific
106: 642–645, 1994 June

Correlated Optical and Radio Structure in the QSO 1302−102[1]

J. B. HUTCHINGS[2] AND S. C. MORRIS

Dominion Astrophysical Observatory, NRC of Canada, 5071 West Saanich Road, Victoria, B.C. V8X 4M6, Canada
Electronic mail: hutchings@dao.nrc.ca, morris@dao.nrc.ca

ANN C. GOWER AND M. L. LISTER[3]

Department of Physics and Astronomy, University of Victoria, P.O. Box 3055, Victoria, B.C. V8W 2Y2, Canada
Electronic mail: agower@otter.phys.uvic.ca

Received 1994 January 10; accepted 1994 April 6

ABSTRACT. We present new optical imaging in two broadband colors of the $z=0.29$ bright QSO 1302−102, obtained with the Wide Field Camera of the *Hubble Space Telescope*. We have performed deconvolution on the *HST* data, previously published CFHT HRCam data, and the combined data. The structure and brightness are measured of an extended knot 2.3 arcsec from the QSO, and also of brighter structure in the inner 1 arcsec of the QSO. We compare the optical structure with new and existing maps of the radio structure from the VLA.[4] The 5 arcsec radio structures lie along the directions of some of the optical components. We discuss the implications.

1. INTRODUCTION

The bright QSO 1302−102 has appeared in several optical and radio studies (e.g., Miller et al. 1992; Boroson and Green 1992; Kellerman et al. 1989; Miller et al. 1993). Optical imaging was most recently reported by Hutchings and Neff (1992, hereafter referred to as HN). In this, we noted the presence of a faint, red, extended knot about 2 arcsec N of the QSO, and some other brighter structure closer in, on the same side of the nucleus. The main structure of the host galaxy is smooth, with a hybrid luminosity profile. Hutchings and Neff (1990) report that the host galaxy luminosity is high, with an absolute magnitude of −23.7. The ratio of nuclear to host luminosity is average to high: the QSO is optically variable, with recorded changes from 14.9 to 16.1 during the 1970s (Bozyan et al. 1990). It has (low) optical polarization in the range 0.08%–0.18% (Berriman et al. 1990). Finally, the optical spectrum shows line properties near the edge of normal for radio-loud QSOs, and compared with most PG QSOs has weaker than normal emission-line equivalent widths, and weaker than normal Hβ to [O III] ratio. These results are generally consistent with some beaming of the optical nuclear flux along the line of sight, although they are not a definitive indication of such an effect.

Radio structure at 20 cm was reported by Gower and Hutchings (1984, hereafter referred to as GH), and shows a small two-sided structure (less than 10 arcsec) resembling a miniature wide-angle-tailed (WAT) source, from a ~1 Jy core which is extended in the direction of the lobes. Lister et al. (1994) find the core to be probably variable, and other published fluxes also indicate a variable core flux between ~600 and 1200 mJy. Indeed, the flux may have increased systematically through this range in the period 1980–1984. The Parkes observations at 2700 and 5000 MHz indicate a flat spectral index with both fluxes at ~1.3 Jy.

A 2 cm map by two of us (MLL and ACG) is unresolved, and 21 cm VLBI reported by HN shows an unresolved 640 mJy core with a 0.1×0.04 arcsec beam. VLBI data at other frequencies (e.g., Morabito et al. 1986), show lower fluxes with smaller beams, which suggest that there may be extended structure down to the few mas level. However, in the absence of simultaneous total flux measurements, the known variability of the source makes it difficult to assess how much flux may be present in extended structure in the 5–50 mas range. The source is not included in the sample of core-dominated sources of Murphy et al. (1993), because of its declination, but it is clearly a similar type. We report in this paper a new 6 cm map of the source, with the VLA in A-configuration. The details of the VLA observations are given in Lister et al. (1994).

Since the QSO is unusual, and has small-scale optical and radio structure, it was observed with the Wide Field Camera on the *HST*. Data were obtained in 1993 August, with two broadband filters: F555W and F702W. These approximately match the *V* and *I* filters used in the CFHT images. Exposures were 800 s with each filter. Sampling is at 0.1 arcsec and the telescope was in nominal fine lock. While the *HST* spherical aberration was a severe problem in studying faint structure near to a bright point source, the *HST* and HRCam data were combined in the hope of improving on each on its own. We used two algorithms of Lucy and Hook to do the deconvolutions: these are the STSDAS tasks "acoadd" and "plucy." The former allows datasets of different PSF to be

[1]Based on observations made with the NASA/ESA *Hubble Space Telescope*, obtained at the Space Telescope Science Institute, which is operated by the Association of Universities for Research in Astronomy, Inc., under NASA contract NAS 5-26555.
[2]Observer with the NASA/ESA *Hubble Space Telescope*, through the Space Telescope Science Institute, which is operated by AURA Inc., under NASA contract NAS 5-26555.
[3]Present address: Dept. of Astronomy, Boston University, 725 Commonwealth Ave., Boston, MA 02215; Electronic mail: lister@bu-ast.bu.edu.
[4]The VLA is part of the National Radio Astronomy Observatory, which is operated by Associated Universities Inc., under contract with the National Science Foundation.

© 1994. Astronomical Society of the Pacific

© Astronomical Society of the Pacific • Provided by the NASA Astrophysics Data System

1994PASP..106..642H

combined. Details of the software may be found in Stobie et al. (1994) and Lucy and Hook (1991).

2. OPTICAL DATA PROCESSING

The HRCam observations used the QSO nuclei as guide stars. This means that the central 1.5 arcsec of the image was attenuated by a factor of 20. Before image restoration, this central part was reconstituted. However, this part of the image is regarded as unreliable in the final image. As an empirical verification, we ran the processing with the unedited image too, to check that the apparent structure outside this area is not significantly affected.

The HRCam observations did not contain a good PSF star in the same frame: one was chosen from another observation on the same run, with similar image quality. The HRCam PSF is noncircular, principally because of astigmatism in the telescope mirror. A Gaussian PSF, fitted to the stellar PSF, was used as an experiment to determine how sensitive the result is to the choice of PSF. It was found that the structure of interest is very little affected by using an artificial PSF of similar shape and size. The advantage of the artificial PSF is that it does not introduce noise, particularly in the outer parts of the profile which is just where we are looking for faint structure in this work. The signal levels in the regions of interest are low, and we found that when using "acoadd," more than about ten iterations of deconvolution generally amplified noise and nonreal features at the expense of those we wished to study. Figure 1 shows the HRCam data deconvolved.

The WFC images were saturated in the central few pixels, which led to charge leakage over five pixels in the central two columns. Before image restoration, these pixels were edited to remove this excess signal. The central 0.3 arcsec was regarded as unreliable in the final images. As for the HRCam data, we did use the unedited images to check that the structure outside this area is not significantly affected by this editing.

The WFC data were deconvolved using artificial PSFs derived from the program Tiny Tim, which takes into account the position within the WFC of the QSO image, and also the filters used, as well as the color of the object. The field contains one bright star. This was unsuitable as a PSF as its structure was clearly different, and the central pixels were saturated. Other stars in the field were much too faint to be useful, and presumably also have different structure. As a useful control we did perform a deconvolution of the star using a Tiny Tim PSF. Once again, to study the structures of interest, only five to ten iterations were useful when using "acoadd." We also obtained some results using the new "plucy" algorithm, whose convergence criteria are different, and required about 100 iterations to satisfy. These results appear to be better for our WFC data, but the algorithm does not allow the addition of the HRCam data. Figure 1 shows WFC images deconvolved.

Finally, the HRCam and WFC data were combined with "acoadd," matching colors in the datasets. The images were registered with each other to fractional-pixel accuracy: the fiducial marks used were the QSO and two nearby galaxies seen in both datasets. The deconvolved images are shown in Fig. 1. In Table 1 we show photometric measures from various images.

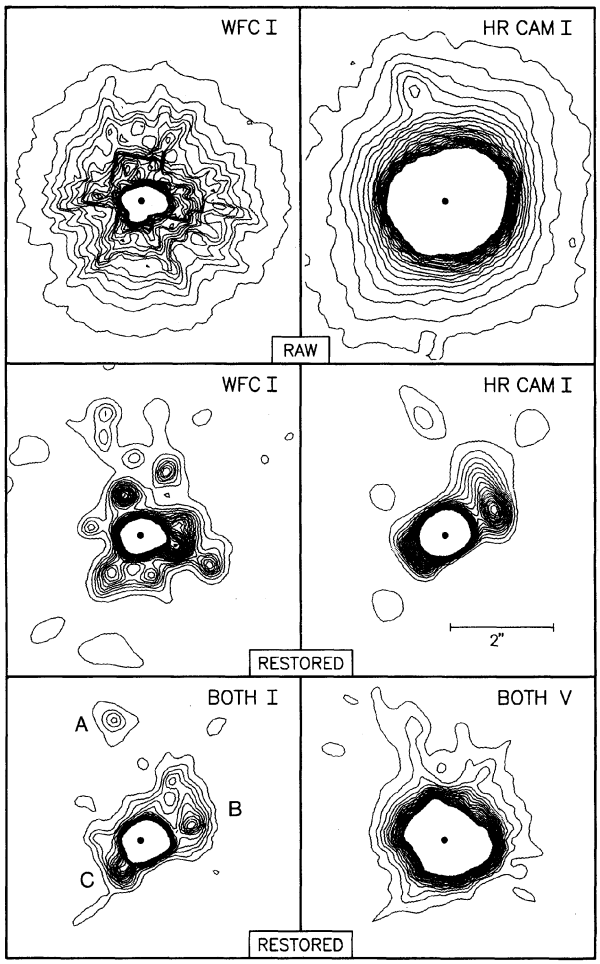

FIG. 1—*HST* and HRCam images and restorations. N is up and E to the left. The contours are linearly spaced and show only the lower signal levels. *Top:* The raw images; *Middle:* WFC deconvolved with plucy 100 iterations and HRCam deconvolved with acoadd ten iterations; *Lower:* combined WFC and HRCam deconvolved with acoadd ten iterations, in two colors. The significant structures can be seen in the HRCam and combined images: in the *HST* data alone there are several PSF features that are spurious. The structures, A, B, C, are redder than the QSO nucleus, and those nearest to the nucleus may also have some spurious structure.

Further experiments to test sensitivity were made by varying the relative peak levels of the WFC and HRCam images, and deliberately misaligning the QSO and PSF. We determined that none of the results we discuss are sensitive to these quantities over ranges significantly larger than their uncertainties.

3. RESTORATION RESULTS

The WFC data on their own are dominated by the PSF, and without the independent knowledge from HRCam, little can be said about the QSO extended structure. However, the faint feature E of N, seen clearly in the HRCam images, is

© Astronomical Society of the Pacific • Provided by the NASA Astrophysics Data System

1994PASP..106..642H

TABLE 1
1302−102 Measured Flux Ratios

Image	Iterations	Filter	Q/total	Q/A	Q/B
HRCam	raw	*I*	0.71	≥110	—
	5		0.91	370	—
	10		0.93	350	30
WFC	raw	F702W	0.27	175	—
	5		0.70	150	18
Both	5	Red	0.87	250	—
	10		0.87	160	23
	20		0.85	160	21
HRCam	raw	*V*	0.56	430	—
	5		0.77	480	—
WFC	raw	F555W	0.23	—	—
	5		0.71	400	—
Both	5	Vis	0.91	400	100

Q=QSO; A=component at 2.3" E of N; B=component<1" NW; Total=all signal within 5" box around QSO.

present and persistent. We call this component A. It does not show up in the WFC star images, and does not change with alignment of the PSF or other alterations in the restoration procedure. However, it is heavily blended with PSF artifacts which never completely disappear.

The HRCam restoration clearly shows this feature, which was measured by HN in the raw data, and also improves the previously noted brighter structure closer in, to the NW. We refer to this as component B. The shape and brightness of this inner feature depends on the details of the restoration procedure, but it is present in some form in all instances. Thus, it seems probable that there is a real feature there. There is some structure at this location in the WFC restored images, although very blended with PSF artifacts.

The most interesting result is in the combined restored image, as it improves details seen in both datasets. The shape and flux of the extended features are fairly robust to the range of reasonable restoration parameters, and iterations. In Table 1 we show measurements of these features in the images. We note that the feature B appears to curve sharply from being radial to point towards feature A, and that feature A is extended in the direction of B. Thus, as HN suggested, the features may be part of a general bent structure that goes in to the nucleus. Finally, we note a third feature (C), which emerges from the nucleus, to the SE. This feature is small and close in, and may not be real.

The more distant faint feature is clearly redder than the QSO nucleus, as was pointed out by HN. The ratio of feature to QSO flux is higher in *I* than *V* for both features we have measured. In making quantitative measures of this, we note that the effect of restoration is to move most of the signal into the nucleus, as seen in column 4 of Table 1. Convergence of this process is not easy to define for this type of object, where we are interested in real faint structure that surrounds the nucleus, and not in removing it all. The NE detached feature is stable to most of the process, but the closer and brighter feature B to the SW is blended with PSF features. Thus, many iterations of restoration may remove flux that should remain in the features we are studying. From all the restorations we did, and the representative values in Table 1, we adopt the ratios 160 and 20 in *I* and 400 and 100 in *V* for the features A and B compared with the QSO. With considerable uncertainty, B appears to be redder than A: A is 1 mag redder in $V-I$ than the QSO and B is perhaps 0.7 mag redder still.

While we have located and measured these two strong features in the QSO fuzz, the overall smooth flux distribution of the QSO host galaxy is seriously affected by the restoration process, and we do not attempt to improve upon it with this process.

4. RADIO STRUCTURE AND DISCUSSION

In Fig. 2 we show our 6 cm radio map, and also a composite sketch based on maps at 6 and 20 cm with the outline of the optical features superposed. The radio structure sketch does not have quantitative contour levels, but does show the core and lobe shapes and high points that are common in all the maps. While the 6 cm lobes are very weak, and their spectral index steep, it is interesting how similar the structures appear at 6 and 20 cm, implying that the spectral index does not vary much along the length of the structure. (An accurate spectral index map is not possible since the UV coverage is not exactly the same at the two wavelengths.) This suggests that the structure is actually small, rather than just severely shortened by projection effects. The core power is in the range of 25.5 in log(W/Hz), while the lobe power is 23.7 at 6 cm and 24.2 at 20 cm. The lobe fluxes of 30 mJy at 20 cm and 10 mJy at 6 cm lead to a spectral index of 0.9, but with an uncertainty of at least 0.3.

The main new point of interest is the correspondence between the optical and ratio structure. The overall QSO host galaxy extends roughly to the lowest radio contours sketched around the core. The NE optical feature A lies along the direction of the main radio lobe, and there is also a possible optical extension (C) along the direction to the SE lobe. We have not measured the optical flux of this feature as it blends heavily with the nucleus, and may be spurious. However, the directional coincidence is suggestive, and does appear in all our restorations. We note also that the lowest radio contours around the core are extended in these directions, so that radio structure exists in these directions close to the core.

The other optical feature (B) has no radio counterpart. However, as noted already, this feature appears to curve and point towards the outer feature A. None of the features are collinear on opposite sides of the nucleus, so that the bending or misalignment occurs very close to the central source.

There are two alternative explanations of the optical structure. The first is that the optical features are parts of an interacting or merging companion, as seen, e.g., in 1229 +204 and 1403+434 in HN. The possible sharp bend in feature B and the red colors argue against this (usually star formation makes such features blue), as well as the alignment with the radio structure. The second possibility is that the optical structure is associated with and even caused by

© Astronomical Society of the Pacific • Provided by the NASA Astrophysics Data System

1994PASP..106..642H

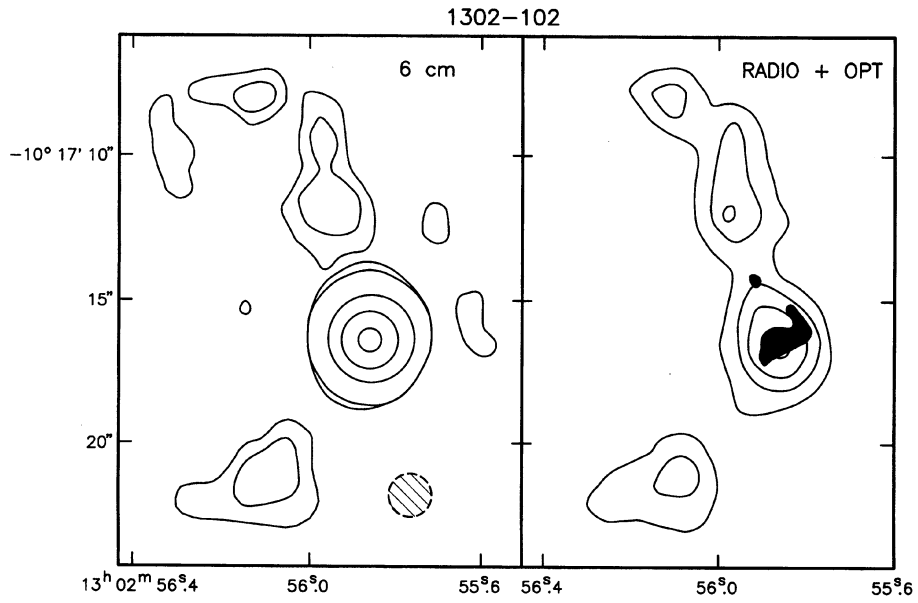

FIG. 2—*Left:* the new 6 cm map. Contour levels are 0.1%, 0.2%, 5%, 30%, and 80% of the peak flux of 982 mJy per beam. *Right:* Sketch showing the shape and high points of the radio structure, based on GH 20 cm map, the new 6 cm map, and a 20 cm map of Perley (private communication). Superposed is the outline of the combined restored red image from Fig. 1. Note the correspondence of the directions of the optical and radio structures.

the radio source, and seems the more likely here. The compact and bent nature of the radio source suggests that it is being affected by radio jet interaction with a dense ISM in the host galaxy. A redirection of the nuclear beam may be what is seen in feature B, which is too small to be seen in the 6 and 20 cm radio maps, and may be too faint to show up in the 2 cm or VLBI data. The formation of bent ("dogleg") sources by such mechanisms is discussed by Stocke et al. (1985).

HN note the smoothness and hybrid luminosity profile of the azimuthally averaged QSO host, in spite of the peculiar features we have discussed. They suggest that the galaxy is a fairly old merger. The small size of the radio source, the correspondence with the optical structure, and the sharp bends in both radio and optical structure suggest that the radio source may just be turning on, and the radio jets just emerging from the host galaxy.

GH suggested the whole source may be a precessing one seen along the cone edge of the approaching beam. However, the suggested sharp bend in optical feature B, as well as the sharp bends now apparent along the radio lobes, argue against that model. A helical path model (e.g., Conway and Murphy 1993) is visually indistinguishable from a ballistic precession and may still have an application here. However, if we assume such models, the sharp bends would imply that we see *both* sides of a two-sided source, with considerable foreshortening, and little beaming of the extended flux. We noted in Sec. 1 that the optical spectrum is consistent with (but not very strongly suggestive of) nuclear beaming that might arise from such a scenario.

While it is not yet possible to distinguish these possibilities, the radio and optical structure of this QSO is unusual, and may be a clue to the early development of the nuclear activity. Further high-resolution imaging in both radio and optical wavelengths is of considerable interest.

We are grateful to Richard Hook for supplying us with early releases of "acoadd" and "plucy." It is a pleasure to thank J.-C. Hsu. Ramon Williamson II, and Nelson Zarate, all of STScI, for help with other components of STSDAS.

REFERENCES

Berriman, G., Schmidt, G. D., West, S. C., and Stockman, H. S. 1990, ApJS, 74, 869
Boroson, T., and Green, R. F. 1992, ApJS, 80, 109
Bozyan, E. P., Hemenway, P. D., and Argue, A. N. 1990, AJ, 99, 1421
Conway, J., and Murphy, D. W. 1993, ApJ, 411, 89
Gower, A. C., and Hutchings, J. B. 1984, AJ, 89, 1658 (GH)
Hutchings, J. B., and Neff, S. G. 1992, AJ, 104, 1 (HN)
Hutchings, J. B., and Neff, S. G. 1990, AJ, 99, 1715
Kellerman, K. I., Sramek, R., Schmidt, M., Shaffer, D. B., and Green, R. 1989, AJ, 98, 1195
Lister, M., Gower, A. C., and Hutchings, J. B. 1994, AJ (preprint)
Lucy, L. B., and Hook, R. N. 1991, ST-ECF Newsletter, 16,6
Miller, P., Rawlings, S., Saunders, R., and Eales, S. 1992, MNRAS, 254, 93
Miller, P., Rawlings, S., and Saunders, R. 1993 MNRAS, 263, 425
Morabito, D. D., Niell, A. E., Preston, R. A., Linfield, R. P., Wehrle, A. E., and Faulkner, J. 1986, AJ, 91, 1038
Murphy, D. W., Browne, I. W. A., and Perley, R. A. 1993, MNRAS, 264, 298
Stobie, E. B., Hanisch, R. J., and White, R. L. 1994, Astronomical Data Analysis Software and Systems III, ASP Conference Series (in press)
Stocke, J. T., Burns, J. O., and Christiansen, W. A. 1985, ApJ, 299, 799

© Astronomical Society of the Pacific • Provided by the NASA Astrophysics Data System